Goulet, J. and Smith, I. (2013). Performance-driven measurement-system design for structural identification. Journal of Computing In Civil Engineering, 27(4):427–436. http://cedb.asce.org

PERFORMANCE-DRIVEN MEASUREMENT-SYSTEM DESIGN FOR STRUCTURAL IDENTIFICATION

James-A. Goulet A. M. ASCE[1] and Ian F. C. Smith, F. ASCE[2]

Abstract

Much progress has been achieved in the field of structural identification due to a better understanding of uncertainties, improvement in sensor technologies and cost reductions. However, data interpretation remains a bottleneck. Too often, too much data is acquired, thus hindering interpretation. In this paper, a methodology is described that explicitly indicates when instrumentation can decreases the ability to interpret data. The approach includes uncertainties along with dependencies that may affect model predictions. Two performance indices are used to optimize measurement system designs: monitoring costs and expected identification performance. A case-study shows that the approach is able to justify a reduction in monitoring costs of 50% compared with an initial measurement configuration.

Keywords: Computer-aided design, Measurement System, Sensor placement, Uncertainties, dependencies, Expected Identifiability, System Identification, Monitoring

INTRODUCTION

Identifying and understanding the behaviour of civil structures based on measurement data is increasingly used for avoiding replacement and strengthening interventions (Catbas et al. 2012). Much progress has been achieved in the field of structural identification due to a better understanding of uncertainties as well as improvements in sensing technologies and data-acquisition systems (Fraser et al. 2010). However, data interpretation remains a bottleneck. Indeed, in many practical situations, the cost of making sense of data often exceeds by many times the initial cost of sensors. Brownjohn (2007) noted that currently, there is a tendency toward over-instrumentation of monitored structures. This challenge often becomes critical when monitoring over long periods. There is a need to determine which measurements are useful to determine the behaviour of a system. Intuitively, engineers measure structures where the largest response is expected. This ensures that the ratio between the measured value

[1]Ph.D. Student, IMAC, École Polytechnique Fédérale de Lausanne (EPFL), School of Architecture, Civil and Environmental Engineering ENAC, Lausanne, Switzerland (corresponding author). E-mail: James.A.Goulet@gmail.com

[2]Professor, IMAC, École Polytechnique Fédérale de Lausanne (EPFL), School of Architecture, Civil and Environmental Engineering ENAC, Lausanne, Switzerland. E-mail: Ian.Smith@epfl.ch

and the measurement error is the largest. However, these locations may not be those that support structural identification in the best way. Furthermore, in the case of structural identification, measurement uncertainties are often not the dominant source of uncertainty (Goulet et al. 2010).

Robert-Nicoud et al. (2005) proposed a multi-model approach combined with an entropy-based sensor-placement methodology. The application of the methodology by Kripakaran and Smith (2009) to a bridge case-study showed that a saturation of the amount of useful information can be expected. At some point, adding sensors did not reduced the number of models that were able to explain measured behaviour. In the field of structural engineering, the concept of entropy-based sensor placement was also explored by other researchers (Yuen et al. 2001; Papadimitriou 2004; Papadimitriou et al. 2005; Papadimitriou 2005). These applications also showed that saturation of the information increased as sensors were added. Many other researchers (Cherng 2003; Kammer 2005; Kang et al. 2008; Liu et al. 2008; Liu and Danczyk 2009) have made proposals that involve maximizing the amount of information contained in dynamic monitoring signals. Sensor placement is an active field of research in domains such as water distribution networks (Krause and Guestrin 2009) and traffic monitoring (Liu and Danczyk 2009). Also, few researchers have used utility-based metrics to design measurement systems. For instance, Pozzi and Der Kiureghian (2011) have proposed economic criteria instead of sensor information accuracy to plan monitoring interventions. These authors observed that the *"value of a piece of information depends on its ability to guide our decisions"*. This supports the idea that measurement systems should be designed according to measurement goals. Currently there is a lack of systematic methodologies to design measurement systems for a range of measurement goals.

An additional limitation of existing approaches is that most do not explicitly account for systematic bias introduced by epistemic uncertainties. Civil-structure models are prone to epistemic errors that arise from unavoidable simplifications and omissions. Epistemic errors often introduce varying systematic bias over multiple prediction locations and prediction quantities. These effects should be explicitly incorporated in the process of designing measurement systems. Recently, Papadimitriou and Lombaert (2012) have explored the influence of error dependencies on measurement-system design. Also, Goulet and Smith (2011b) proposed an identification methodology that includes systematic bias and epistemic uncertainty dependencies. The methodology was used for predicting the usefulness of monitoring for identifying the parameters characterizing the behavior of a bridge structure (Goulet and Smith 2012). However, the potential of this methodology for optimizing measurement systems was not explored.

This paper proposes a computer-aided measurement-system design methodology that includes systematic bias and epistemic uncertainties. The objective functions used by the methodology includes, the capacity to falsify models and measurement-system cost. The first section summarizes the error-domain model-falsification methodology

and the *expected identifiability* performance metric. The following section describes the measurement-system design methodology and a case-study is presented in the last section.

PREDICTING THE PERFORMANCE OF MEASUREMENT SYSTEMS AT FALSIFYING MODELS

Starting with the principle that observations can best support the falsification of hypotheses, the error-domain model-falsification approach (Goulet et al. 2010; Goulet and Smith 2011b) uses measurements to falsify model instances. A *model instance* is defined as a set of n_p parameters $\boldsymbol{\theta} = [\theta_1, \theta_2, \ldots, \theta_{n_p}]$ characterizing the behaviour of a structural model. These parameters are usually associated with boundary conditions, material properties and the geometry of a structure. Model instances are falsified if at any location i, the difference between predicted $(\mathbf{g}_i(\boldsymbol{\theta}))$ and measured (y_i) values lies outside the interval defined by threshold bounds $(T_{i,Low}, T_{i,High})$ that are based on modeling and measuring uncertainties. Models are falsified if the condition presented in Equation 1 is not satisfied. In this Equation, n_m is the number of measurements.

$$\forall i = 1, \ldots, n_m : \; T_{i,Low} \leq \mathbf{g}_i(\boldsymbol{\theta}) - y_i \leq T_{i,High} \tag{1}$$

The combined uncertainty distribution and its threshold bounds are presented in Figure 1. This distribution is obtained by evaluating modelling and measuring uncertainty sources separately and then combining them together. Details regarding numerical uncertainty combination techniques are presented in ISO guidelines (2008). Threshold bounds define the smallest intervals that include a probability content $\phi \in]0, \ldots, 1]$, defined by users. Details regarding computation of threshold bounds are presented in Goulet and Smith (2012).

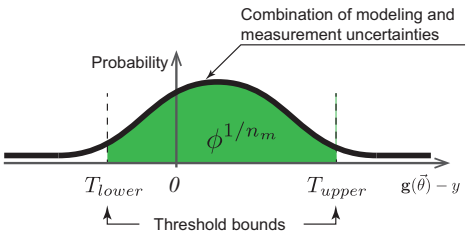

Figure 1. Threshold bounds based on modeling and measuring uncertainties

When n_m measurements are used, it is conservative to define threshold bounds to include a probability content $\phi' = \phi^{1/n_m}$ for the combined uncertainty associated with each comparison point. A *comparison point* is a location where predicted and measured values are compared. Each time a measurement is added, threshold bounds are

adjusted (widened) to include the additional possibility of wrongly falsifying a correct model instance. This is illustrated in Figure 2, where the combined uncertainty for two comparison points are presented in a multivariate probability density function (*pdf*). The projection of threshold bounds including a probability ϕ', determined for each combined uncertainty *pdf*, defines a square region that includes a probability content ϕ. Thus, if for any comparison point, the difference between predicted and measured value falls outside this region, the model instance is discarded with a probability $\leq 1 - \phi$ of performing a wrong diagnosis (discarding a correct model). Šidák (1967) noted that this procedure lead to conservative threshold bounds regardless of the dependency between the random variables that are used to represent uncertainties.

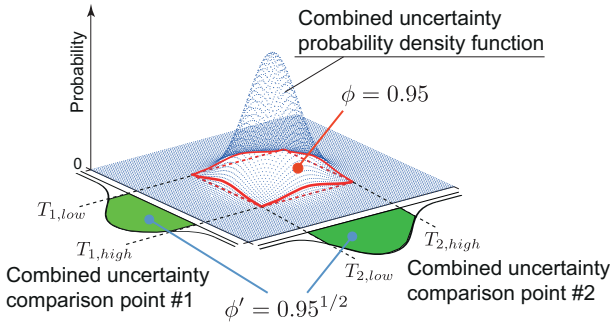

Figure 2. Threshold bounds based on model and measurement uncertainties

Prior to measuring a structure, simulated measurements are generated by subtracting error samples taken in the combined uncertainty distribution from the predictions given by a model instance. Dependencies between prediction uncertainties are included in the process of simulating measurements. These dependencies are described by correlation coefficients. Since little information is available for quantifying these coefficients, a qualitative reasoning formulation is used to describe them. In this formulation, uncertainty correlations are described qualitatively by the labels “low”, “moderate” and “high”, and by labels “positive” or “negative”. These labels correspond to a probability distribution for the correlation value as presented in Figure 3. Each probability density function defines the frequency of the uncertainty correlation values used during the generation of simulated measurements.

Before measuring, an infinite number of parameter sets $\boldsymbol{\theta}$ might be acceptable explanations of the structure behavior. The space of possible solutions is represented by a finite number of model instances. These instances are organized in a n_p-parameter grid that is used to explore the space of possible solutions. Such a grid is named the *initial model instance set*. An example is presented in Figure 4 for two parameters.

For a measurement and load-case configuration, the goal is to predict probabilistically the expected number of candidate models that should remain in the set if real

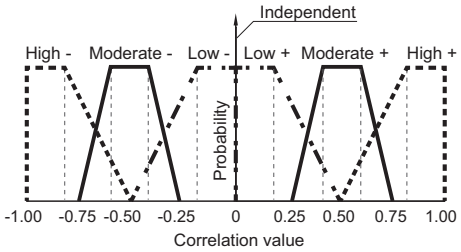

Figure 3. Qualitative reasoning formulation used to include the uncertainty associated with uncertainty dependencies Reprinted from Goulet and Smith (2012) with permission from ASCE

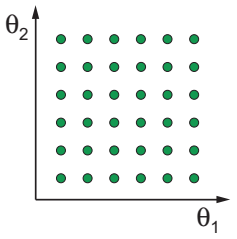

Figure 4. Initial model set organized in a n-parameter grid used to explore the space of possible solutions

measurements are taken. The number of candidate models (n_{CM}) obtained from each instance of simulated measurements is stored in a vector $\boldsymbol{\Upsilon}_{CM}$. Results contained in this vector are summarized in an empirical cumulative distribution function (*cdf*, $F_{\Upsilon_{CM}}(n_{CM})$). This *cdf* describes the certainty of obtaining any number of *candidate models* if measurements are taken on the structure. The quantity extracted from the *cdf* is the maximal number of expected candidate models that should be obtained for a 95% certainty ($F^{-1}_{\Upsilon_{CM}}(0.95)$). F^{-1} represents the inverse *cdf*. An example of $F_{\Upsilon_{CM}}$ is presented in Figure 5 where the horizontal axis corresponds to the expected size of the candidate model set and the vertical axis to the certainty of obtaining a maximum candidate model set size. In this example, there is a certainty of 95% of falsifying at least 60% of the models ($F^{-1}_{\Upsilon_{CM}}(0.95) \approx 40\%$). This quantity is defined as the *expected identifiability* and can be used for predicting the ability of measurement systems to falsify model instances.

The predictive capacity of this approach was validated by Goulet and Smith (2012) in a full-scale study using real data. It was show that the expected identifiability metric can adequately predict the number of candidate model that should be obtained when using real measurement data.

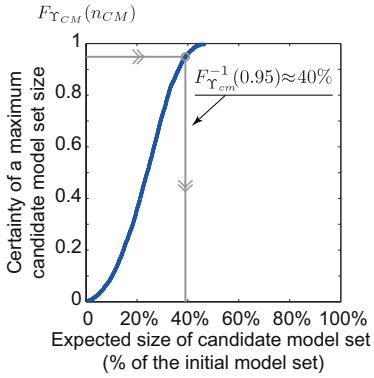

Figure 5. Example of how the performance of a measurement system is computed using the number of candidate models obtained from simulated measurements

MEASUREMENT-SYSTEM DESIGN

The expected identifiability described in the previous section is used as a performance metric to optimize the efficiency of measurement systems. Moreover, in common monitoring interventions, a balance is sought between performance and cost. Therefore, the methodology also uses measurement-system cost as a second objective for optimizing measurement systems. The cost of a measurement system is computed to be the sum of sensor costs and the expenses related to testing equipment, such as trucks in the case of static-load tests. It is assumed that the manpower required during measurements is constant.

In order to maximize the monitoring efficiency, the performance of several measurement and load configurations are studied. There are complexity issues involved with optimizing the performance of measurement systems. Equation 2 presents the number of possible sensor configurations. When selecting configurations involving 20 measurements there are more than a million possibilities. For 300 measurements, the number of possibilities is $\approx 10^{90}$.

$$\sum_{k=1}^{n_m} \frac{n_m!}{k!(n_m-k)!} = 2^{n_m} - 1 \tag{2}$$

This illustrates the exponential growth of the solution space with the number of measurements. In order to obtain optimized solutions efficiently, advanced search algorithms are necessary. Several stochastic global search algorithms are available in the literature (Deb et al. 2002; Raphael and Smith 2003; Kirkpatrick et al. 1983; Kennedy and Eberhart 1995; Cormen 2001) with several applications in the field of civil engineering (Harp et al. 2009; Dimou and Koumousis 2009; Domer et al. 2003). In this paper, a greedy optimization methodology is chosen because it is particularly suited

to the characteristics of this task. Further discussion is provided later in this paper. Note that the approach presented is not limited to the optimization algorithm chosen to explore measurement-system configurations.

Methodology

The methodology used to design efficient measurement systems is based on a Greedy algorithm. At each iteration, it identifies the measurement that can be removed from an initial configuration containing N measurements while minimizing the expected number of candidate models. This process is repeated until a single measurement and load case is left.

Figure 6 presents a flowchart summarizing steps described above for optimizing the performance of measurement systems. In this flowchart, the vector $\boldsymbol{s}$ contains n_m dummy variables indicating whether or not a potential measurement location is used. The Greedy algorithm first evaluates the expected identifiability when using simultaneously all possible measurement types and locations. Once, the expected identifiability ($F^{-1}_{\Upsilon_{CM}}(0.95)$) is computed, each sensor is removed from the set of $N = n_m$ selected sensors, $\boldsymbol{s}(i) = 0 \; \forall i \in \{1, \ldots, N\}$. The sensor removal leading to the best performance is removed permanently from the set of selected sensors. This process is repeated iteratively with $N = N - 1$ sensors until a single sensor is left. In the case of static measurements, it is useful to optimize simultaneously the number of sensors and load-cases used. Therefore, the algorithm stops when a single sensor and load-case are obtained. The cost associated with each solution is computed and non-optimal solutions (with respect to cost) are removed. The results from measurement-system optimization are returned in a two-objective graph as presented in Figure 6 and in a table containing the details of each measurement-system configuration.

Users may then choose the measurement system that is the best tradeoff between the expected performance and available resources. If the expected performance cannot justify monitoring interventions, new measurement locations and types may be evaluated. If such possibilities do not exist, this operation could lead to a justification for performing no monitoring on the structure, thereby redirecting monitoring resources to other structures where data would be more useful to understand system behavior.

Figure 7 schematically presents an example of the trends of two competing factors in measurement-system design. The number of measurements used is the horizontal axis and the expected number of candidate models is the vertical axis. This last quantity is expressed as a percentage of the initial model set size expected for a certainty of 0.95. Note that the number of measurements used is in many cases proportional to the monitoring cost. These curves describe the relationships between the expected number of models and the number of sensors used.

In Figure 7 the total number of candidate models (solid line) decreases as the number of measurements increases, until the point where additional observations are not useful. Beyond this point, additional measurements may decrease the efficiency of the identification by increasing the number of candidate models (i.e. reducing the number

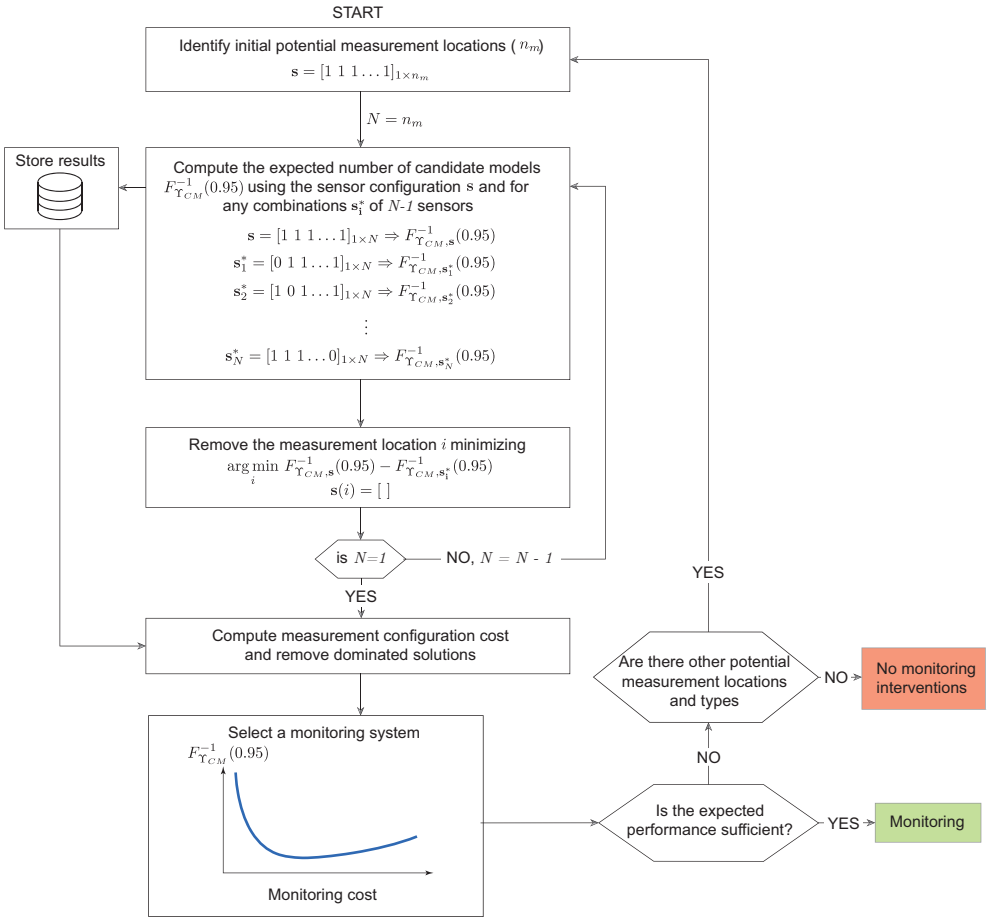

Figure 6. Flowchart schematically representing steps involved in optimizing the performance of measurement systems.

of falsified models). Over-instrumentation is due to the combined effects of an increase in performance due to additional information brought by new observations and a decrease in performance due to threshold adjustments (dashed lines).

In order to avoid over-falsification, threshold bounds are conservatively adjusted using the Šidák correction. Threshold corrections ensure that the reliability of the identification meets the target ϕ when multiple measurements are used simultaneously to falsify model instances. In other words, the criterion used to falsify models (threshold bounds) depends upon the number of measurements used. Over-instrumentation occurs when including a new measurement falsifies less model instances than the number of additional instances accepted due to threshold bound adjustments. Such a situation is likely to happen when the information contained in several measurements is not independent. Furthermore, poor identification performance can be expected when

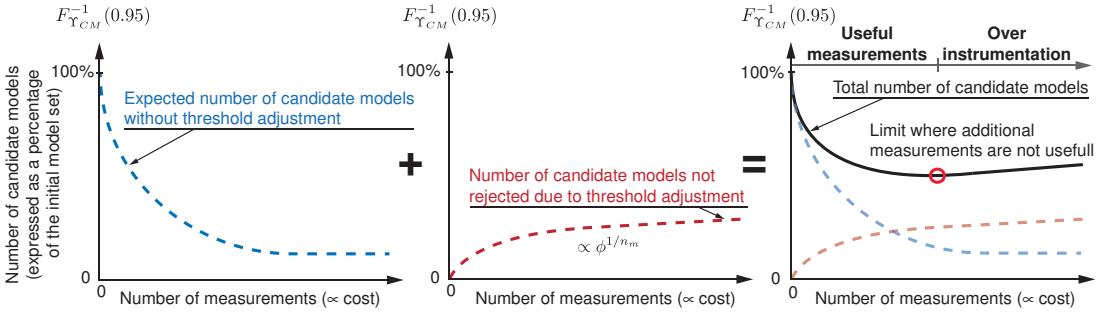

Figure 7. Schematic representation of the phenomena involved in the design of measurement systems. The total number of candidate models decreases as the number of measurements increases until the point where additional observations are not useful (solid curve). Over-instrumentation is due to the combined effects of the increased amount of information and threshold adjustments (dashed curves).

modeling and measuring uncertainties are large in comparison with the prediction variability within the initial model set.

Complexity

For static monitoring, if one load case is possible, the Greedy algorithm performs the measurement-system optimization in less than $n_m^2/2$ iterations, where n_m is the maximal number of measurements. Figure 8 compares the number of iterations required with the number of sensor combinations possible for one load-case. It shows that Greedy algorithm complexity ($O(n^2)$) leads to a number of sensor combinations to test that is significantly smaller than the number of possible combinations ($O(2^n)$).

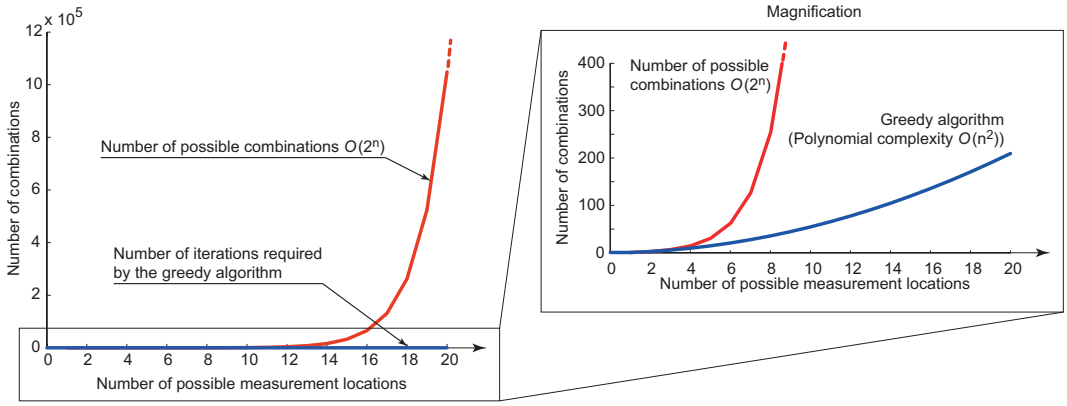

Figure 8. An example of the growth in the number of iterations required by the Greedy algorithm compared with the solution space growth.

CASE-STUDY

The measurement-system design methodology presented in the previous section is used to optimize the monitoring system for investigating the behavior a full-scale structure using static load-tests. The Langensand Bridge is located in Lucerne, Switzerland. Its longitudinal profile is presented in Figure 9.

Case-study description

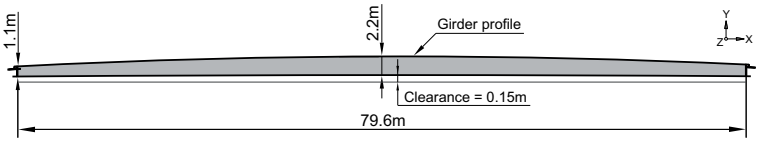

Figure 9. Langensand Bridge elevation representation. Reprinted with permission from the ASCE

The finite-element template model used to generate model instances is presented in Figure 10. The primary parameters to identify are the concrete Young's modulus for the slab poured during construction phase one and two, the asphalt Young's modulus for phase one and two and the stiffness of the horizontal restriction that could take place at the longitudinally free bearing devices. Details of the construction phases are presented in Figure 11. The possible range for concrete Young's modulus varies from 15 GPa to 40 GPa, from 2 GPa to 15 GPa for asphalt, and the bearing device restriction varies from 0 kN/mm to 1000 kN/mm. Each parameter range is subdivided into five intervals to generate 3,125 initial model instances.

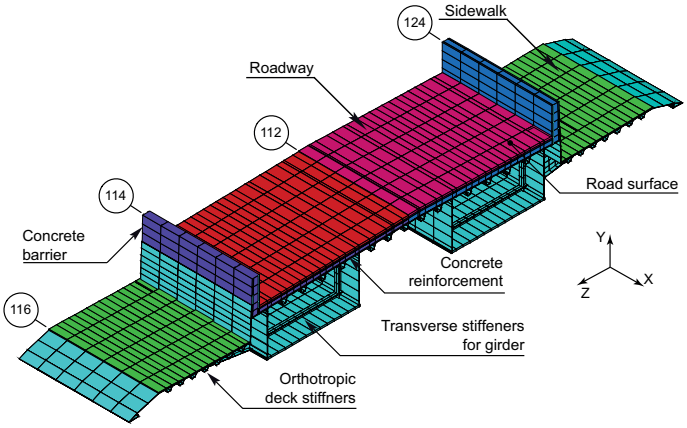

Figure 10. Bridge cross-section detail

The initial measurement system to be optimized is composed of ten displacement, four rotation and five strain sensors. The displacement and rotation measurements are

referenced by the prefix UY for vertical displacement, RZ for the rotation around the transverse axis and EX for strain along the longitudinal axis. The location of each sensor is referenced according to the axes presented in Figure 11. The structure can be loaded using four load-cases presented in Figure 12. Each test-truck weighs 35 tons and each test load-case takes two hours.

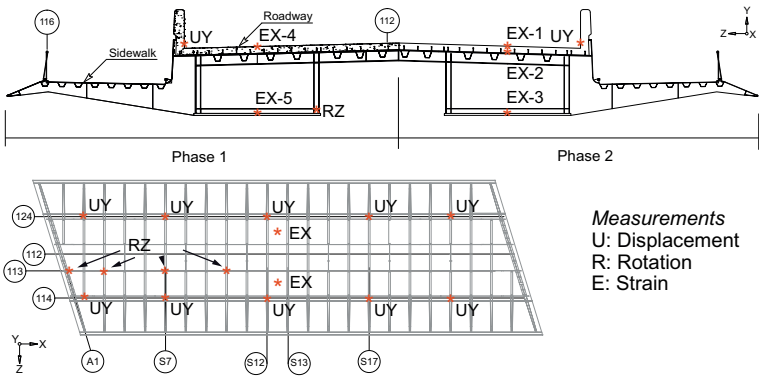

Figure 11. Langensand Bridge cross-section and sensor layout

Each displacement sensor costs US$ 200. Rotation sensors cost US$ 600 each and strain sensors costs US$ 1500 per unit (optical-fiber devices), including installation costs. Test-truck rental is US$ 400 per truck plus an additional US$ 200 per hour of use.

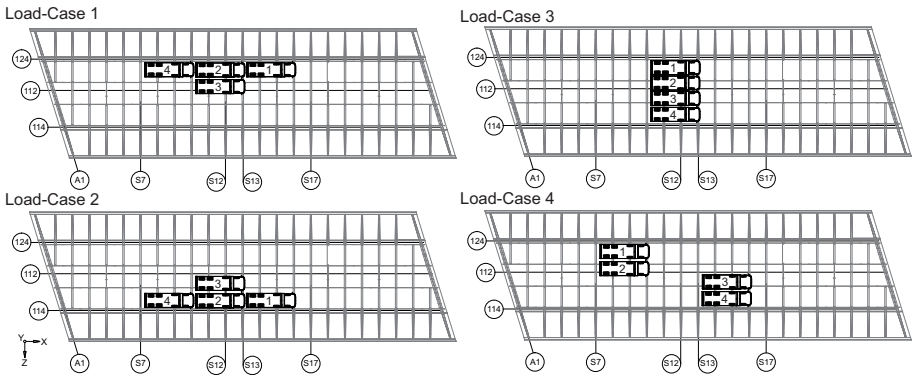

Figure 12. Load-case layout

Modeling and measurement uncertainties

Several random and epistemic uncertainty sources affect the interpretation of data. Table 1 summarizes uncertainties associated with secondary model-parameters that

are not intended to be identified because their effect on predicted response is too small. These are described by Gaussian distributions. The symbol Δ indicates a variation with respect to the nominal value specified for the structure. These uncertainties are propagated in the finite-element template model to obtain the uncertainties related to model predictions.

Table 1. Secondary parameter uncertainties

Uncertainty source	Unit	Mean	σ
Steel Young's modulus	GPa	202	6
Poisson's ration concrete	-	0	0.025
Δ thickness - steel plates	%	0	1
Δ thickness- pavement	%	0	5
Δ thickness- concrete	%	0	2.5
Test-truck weight	Ton	35	0.125
Strain sensor vertical positioning	mm	0	5

Other modeling and measurement uncertainty sources are described in Table 2. These numbers are based on uncertainties defined by Goulet and Smith (2012) for a first study performed on the structure during its construction phase. The probability distribution used to describe three uncertainty sources (model simplifications, mesh refinement and additional uncertainties) is the extended uniform distribution (Goulet and Smith 2011a). This distribution is made of several orders of uniform distribution, each representing the uncertainty associated with the bound position. The intervals defined in Table 2 are the minimal and maximal uncertainty bounds expressed as a percentage of the mean model prediction. These numbers were defined during a first study of the structure during its construction phase (Goulet and Smith 2012). For displacement and rotation predictions, the uncertainty associated with bounds is 30% ($\beta = 0.30$). In the case of strain, this uncertainty is 50% ($\beta = 0.50$) because of local inaccuracies in the bridge model have a more important effect on predicted values.

Sensor resolutions are described by traditional uniform distributions based on manufacturer specifications. Measurement repeatability uncertainty is taken to be Gaussian where the coefficients of variations are estimated to be 1% for displacement measurements, 0.5% for rotations and 3% for strains. These numbers are conservative upper bounds of results obtained from previous measurements (Goulet et al. 2010).

For each uncertainty source presented in Table 2, a qualitative description of uncertainty dependency is provided. In addition, the level of uncertainty correlation between load cases is assumed to be high and positive. The correlation between predictions originating from secondary-parameter uncertainties is implicitly provided when uncertainties are propagated through the finite-element template model. For each measurement location, a combined uncertainty *pdf* is computed. Threshold bounds are

Table 2. Other uncertainty sources

Uncertainty source	Displacement		Rotation		Strains		Qualitative
	min	max	min	max	min	max	correlation
Sensor resolution	-0.2mm	0.2mm	-4μrad	4μrad	-4$\mu\epsilon$	4$\mu\epsilon$	low+
Model simplifications & FEM	0 %	7%	0%	7%	0%	20%	high+
Mesh refinement	-1%	0%	-1%	0%	-2%	0%	high+
Additional uncertainties	-1%	1%	-1%	1%	-1%	1%	moderate+
	mean	σ	mean	σ	mean	σ	
Measurement repeatability	0 %	1%	0%	0.5%	0%	3%	high+

determined for a target probability fixed at $\phi = 0.95$. The definition of the threshold bounds width depends on the number of measurements used in the falsification process. Therefore, specific threshold bounds are computed for each sensor configuration.

Measurement-system design results

Measurement-system optimization is performed according to two criteria: load-test costs and the expected number of candidate models. Both objectives need to be minimized. Results are presented in Figure 13. Load-test costs are presented on the horizontal axis and the expected number of candidate models on the vertical axis. The expected number of models is expressed as a percentage of the initial model set. Each dot represents the optimal measurement-system found for each cost. When using cheap measurement systems with few sensors, poor results are expected. By choosing optimized sensors and test configurations, the performance can be improved for a marginal cost increase. Beyond a certain point, adding sensors and load cases not only stops improving the monitoring efficiency, it decreases it. This quantitatively shows a principle, intuitively known by engineers, that too much measurement data may hinder interpretation.

The sensor and load-case configurations associated with each dot in Figure 13 are reported in Table 3. In this table, the columns containing diamond signs indicate which sensors and load-cases are selected for each configuration reported in Figure 13. The expected number of candidate models is obtained for a certainty of 95%. This is the upper bound for the number of candidate models that should be obtained when using real measurements. This means that individual results are likely to be better.

In this case, the best measurement system found uses 4 sensors with 3 load-cases and would result in almost 80% of model instances to be falsified. This measurement-system configuration is halfway between the cheapest and most expensive measurement systems. It leads to a reduction of monitoring costs by up to 50% compared with the maximal cost.

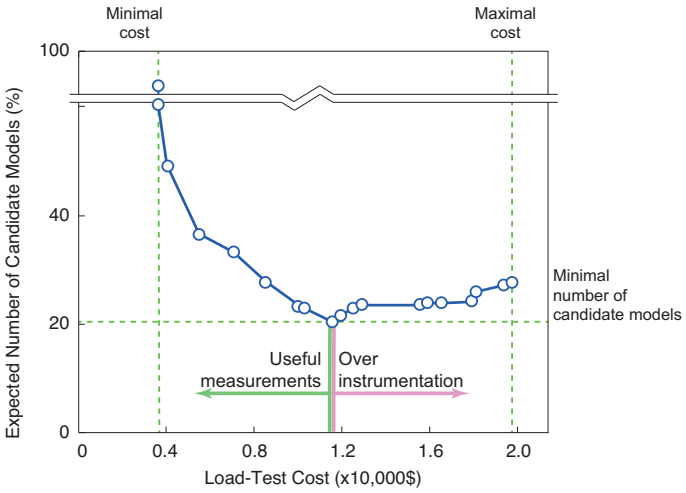

Figure 13. Multi-objective optimization results for the Langensand Bridge.

Table 3. Optimized measurement configurations are shown by a vertical set of symbols ◇ for a given sensor type and location. The cost of the load-test along with the expected number of candidate models computed for certainty of 95% are reported for each configuration.

Sensors & load-cases	Load-test configurations																		
UY-S03-114	◇																		◇
UY-S07-114											◇	◇	◇	◇	◇	◇	◇	◇	◇
UY-S12-114											◇	◇	◇	◇	◇	◇	◇	◇	◇
UY-S17-114														◇	◇		◇	◇	◇
UY-S21-114		◇						◇		◇	◇	◇	◇	◇	◇	◇	◇	◇	◇
UY-S03-124														◇	◇	◇	◇	◇	◇
UY-S07-124											◇		◇	◇	◇	◇	◇	◇	◇
UY-S12-124													◇	◇	◇	◇	◇		◇
UY-S17-124													◇	◇	◇	◇	◇	◇	◇
UY-S21-124											◇	◇	◇	◇	◇	◇	◇	◇	◇
RZ-A1-113			◇	◇	◇	◇	◇	◇	◇	◇	◇	◇	◇	◇	◇	◇	◇	◇	◇
RZ-S4-113												◇	◇	◇	◇	◇	◇	◇	◇
RZ-S7-113													◇	◇	◇	◇	◇	◇	◇
RZ-S10-113															◇	◇	◇	◇	◇
EX-L1													◇	◇	◇	◇	◇	◇	◇
EX-L2						◇	◇	◇	◇	◇	◇	◇	◇	◇	◇	◇	◇	◇	◇
EX-L3																		◇	◇
EX-L4							◇		◇	◇	◇	◇	◇	◇	◇	◇	◇	◇	◇
EX-L5				◇	◇	◇	◇	◇	◇	◇	◇	◇	◇	◇	◇	◇	◇	◇	◇
LC1	◇	◇	◇	◇	◇	◇	◇	◇	◇	◇	◇	◇	◇	◇	◇	◇	◇	◇	◇
LC2								◇	◇	◇	◇	◇	◇	◇	◇	◇	◇	◇	◇
LC3					◇	◇	◇	◇	◇	◇	◇	◇	◇	◇	◇	◇	◇	◇	◇
LC4															◇	◇	◇	◇	◇
Cost (X1000 US $)	3.4	3.4	3.8	5.3	6.9	8.4	9.9	10.2	11.5	11.7	12.5	12.9	15.6	16	16.6	18	18.2	19.5	19.9
Expected CM	3000	1252	1092	909	861	783	722	712	676	694	711	720	720	725	725	729	755	773	781

DISCUSSION

Results presented here indicate that over-instrumenting a structure is possible. This approach is not intended to replace engineering judgment; it is presented as a tool for exploring the benefits of a wide selection of possible sensor types and their locations. In the case where the optimal configuration uses few sensors, additional provisions might be justified to account, through redundancy, for possible sensor breakage and malfunction.

The methodology presented in this paper can be used with optimizations methodologies other than the Greedy algorithm. As it was already noted by (Goulet and Smith 2011c) the global trend of over instrumentation is independent of the optimization technique. This is verifiable because the right end of the curve presented in Figure 13 corresponds to the configuration using all sensors and load cases. In future studies, the optimality of the solution found using a Greedy algorithm could be compared with other stochastic global optimization approaches. If better solutions are found, these will further increase the over instrumentation trends illustrated in this paper. Furthermore, for this case, a sensitivity analysis has shown that the effect of single sensor removal is dominant over the effect of the interaction caused by multiple sensor removal. Therefore, stochastic search algorithms are not expected to provide better optimization results. Aside from the optimization algorithm choice, the shape of the curve obtained from the multi-objective optimization exercise depends on characteristics such as sensor costs, uncertainties as well as possible sensor types and locations.

CONCLUSIONS

Computer-aided measurement-system design supports cost minimization while maximizing expected efficiency identifying the behaviour of structures. Specific conclusions are:

1. The criteria used to falsify models (threshold bounds) are dependent upon the number of measurements. If too many measurements are used, data-interpretation can be hindered by over-instrumentation.
2. The measurement-system design methodology can be used to determine good tradeoffs with respect to interpretation goals and available resources.
3. The approach may prevent over-instrumentation. Furthermore, it indicates situations where measuring a structure is not likely to be useful.

Further work is under way to establish the usefulness of greedy sensor removal with respect to stochastic search methods for a range of cases.

ACKNOWLEDGEMENTS

Collaboration with the designers of the Langensand Bridge - Gabriele Guscetti and Claudio Pirazzi and with the city of Lucerne, was important for successful completion of this research. This research is funded by the Swiss National Science Foundation under contract no. 200020-117670/1.

References

Brownjohn, J. (2007). "Structural health monitoring of civil infrastructure." *Philosophical Transactions of the Royal Society A-Mathematical Physical and Engineering Sciences*, 365(1851), 589–622.

F. Catbas, T. Kijewski-Correa, and A. Aktan, eds. (in press, 2012). *Structural Identification of Constructed Facilities. Approaches, Methods and Technologies for Effective Practice of St-Id*. American Society of Civil Engineers (ASCE).

Cherng, A. (2003). "Optimal sensor placement for modal parameter identification using signal subspace correlation techniques." *Mechanical Systems and Signal Processing*, 17(2), 361–378.

Cormen, T. (2001). *Introduction to algorithms*. The MIT press, Cambridge, MA.

Deb, K., Pratap, A., Agarwal, S., and Meyarivan, T. (2002). "A fast and elitist multiobjective genetic algorithm: Nsga-ii." *IEEE Transactions on Evolutionary Computation*, Vol. 6. 182 –197.

Dimou, C. and Koumousis, V. (2009). "Reliability-based optimal design of truss structures using particle swarm optimization." *Journal of Computing in Civil Engineering*, 23(2), 100–110.

Domer, B., Raphael, B., Shea, K., and Smith, I. (2003). "A study of two stochastic search methods for structural control." *Journal of Computing In Civil Engineering*, 17(3), 132–141.

Fraser, M., Elgamal, A., He, X., and Conte, J. (2010). "Sensor network for structural health monitoring of a highway bridge." *Journal of Computing in Civil Engineering*, 24(1), 1–11.

Goulet, J., Kripakaran, P., and Smith, I. (2010). "Multimodel structural performance monitoring." *Journal of Structural Engineering*, 136(10), 1309–1318.

Goulet, J. and Smith, I. (2011a). "Extended unifiorm distribution accounting for uncertainty of uncertainty." *International Conference on Vulnerability and Risk Analysis and Management/Fifth International Symposium on Uncertainty Modeling and Analysis*, Maryland, USA. 78–85.

Goulet, J. and Smith, I. (2011b). "Overcoming the limitations of traditional model-updating approaches." *Proceedings of the ICVRAM and ISUMA conference*, Maryland, USA. 905–913.

Goulet, J. and Smith, I. (2011c). "Prevention of over-instrumentation during the design of a monitoring system for static load tests." *Proceedings of the 5th International Conference on Structural Health Monitoring on Intelligent Infrastructure (SHMII-5)*, Cancun, Mexico. 80.

Goulet, J. and Smith, I. (In press, 2012). "Predicting the usefulness of monitoring for identifying the behaviour of structures." *Journal of Structural Engineering*.

Harp, D., Taha, M., Eng, P., Ross, T., et al. (2009). "Genetic-fuzzy approach for modeling complex systems with an example application in masonry bond strength prediction." *Journal of Computing in Civil Engineering*, 23(3), 193–200.

JCGM (2008). "Guide to the expression of uncertainty in measurement supplement 1: Numerical methods for the propagation of distributions." *Report No. ISO/IEC Guide 98-3:2008/Suppl 1:2008*.

Kammer, D. (2005). "Sensor set expansion for modal vibration testing." *Mechanical Systems and Signal Processing*, 19(4), 700–713.

Kang, F., Li, J., and Xu, Q. (2008). "Virus coevolution partheno-genetic algorithms for optimal sensor placement." *Advanced Engineering Informatics*, 22(3), 362–370.

Kennedy, J. and Eberhart, R. (1995). "Particle swarm optimization." *Proceedings of IEEE International Conference on Neural Networks*, Vol. 4, IEEE. 1942–1948.

Kirkpatrick, S., Gelatt, C., and Vecchi, M. (1983). "Optimization by simulated annealing." *science*, 220(4598), 671–679.

Krause, A. and Guestrin, C. (2009). "Optimizing sensing: From water to the web." *Computer*, 42(8), 38–45.

Kripakaran, P. and Smith, I. (2009). "Configuring and enhancing measurement systems for damage identification." *Advanced Engineering Informatics*, 23(4), 424–432.

Kuehl, R. (2000). *Design of experiments: statistical principles of research design and analysis*. Duxbury/Thomson Learning, Pacific Grove, CA.

Liu, H. and Danczyk, A. (2009). "Optimal sensor locations for freeway bottleneck identification." *Computer-Aided Civil and Infrastructure Engineering*, 24(8), 535–550.

Liu, W., Gao, W., Sun, Y., and Xu, M. (2008). "Optimal sensor placement for spatial lattice structure based on genetic algorithms." *Journal of Sound and Vibration*, 317(1-2), 175–189.

Papadimitriou, C. (2004). "Optimal sensor placement methodology for parametric identification of structural systems." *Journal of sound and vibration*, 278(4-5), 923–947.

Papadimitriou, C. (2005). "Pareto optimal sensor locations for structural identification." *Computer methods in applied mechanics and engineering*, 194(12-16), 1655–1673.

Papadimitriou, C., Haralampidis, Y., and Sobczyk, K. (2005). "Optimal experimental design in stochastic structural dynamics." *Probabilistic engineering mechanics*, 20(1), 67–78.

Papadimitriou, C. and Lombaert, G. (2012). "The effect of prediction error correlation on optimal sensor placement in structural dynamics." *Mechanical Systems and Signal Processing*, 28, 105—127.

Pozzi, M. and Der Kiureghian, A. (2011). "Assessing the value of information for long-term structural health monitoring." *Proceedings of SPIE*, Vol. 7984.

Raphael, B. and Smith, I. (2003). "A direct stochastic algorithm for global search." *Applied Mathematics and Computation*, 146(2-3), 729–758.

Robert-Nicoud, Y., Raphael, B., and Smith, I. (2005). "Configuration of measurement systems using shannon's entropy function." *Computers & Structures*, 83(8-9), 599–

612.

Šidák, Z. (1967). "Rectangular confidence regions for the means of multivariate normal distributions." *Journal of the American Statistical Association*, 62, 626–633.

Yuen, K., Katafygiotis, L., Papadimitriou, C., and Mickleborough, N. (2001). "Optimal sensor placement methodology for identification with unmeasured excitation." *Journal of dynamic systems, measurement, and control*, 123, 677–686.